

Yan-tao Yu, Jin-hui Peng*, Bing-guo Liu, Guo Chen and C. Srinivasakannan

Investigation on Preparation of Micro-Sized Hematite Powder from Hydrous Ferrous Sulfate Using Microwave and Conventional Heating

Abstract: Microwave and conventional heating were employed to synthesize micro-sized hematite powder from hydrous ferrous sulfate, a by-product in the process of titanium pigment manufacture. The TG/DTG analysis was used to study thermal behavior of the industrial ferrous sulfate. Therefore the temperature which was significant to product was defined. The calcination experiments were carried out to assess the effect of calcination temperature covering three different temperatures (650°C, 750°C and 850°C, respectively). X-ray powder diffraction (XRD) was used to characterize the structure of the product, while the scanning electron microscopy (SEM) was utilized to characterize the morphology of the product. Microwave calcination process resulted in a mixture of hematite and minor magnetite while a considerable amount of magnesium sulfate was detected with the conventional calcination process. The transformation from periclase to magnesium was discussed during the calcinations as well. The conventional heating resulted in porous product while the microwave heating resulted in smaller particle size.

Keywords: hematite, microwave, calcinations, ferrous sulfate

PACS® (2010). 81.20.Ka

***Corresponding author: Jin-hui Peng:** Key Laboratory of Unconventional Metallurgy, Ministry of Education, Faculty of Metallurgical and Energy Engineering, Kunming University of Science and Technology, Kunming 650093, China
E-mail: jhpeng@kmust.edu.cn

Yan-tao Yu, Bing-guo Liu, Guo Chen: Key Laboratory of Unconventional Metallurgy, Ministry of Education, Faculty of Metallurgical and Energy Engineering, Kunming University of Science and Technology, Kunming 650093, China
C. Srinivasakannan: Chemical Engineering Department, The Petroleum Institute, Abudhabi, UAE

1 Introduction

Micro-sized hematite powder is one of the most important inorganic nonmetallic materials that provide large surface area. Hematite has been used in diverse applications which include magnetic materials [1], pigment [2], sensors [3], catalyst [4], drug carriers for magnetically guided drug delivery [5] etc. Ferrous sulfate, a byproduct of titanium pigment production through sulfuric acid process, could be utilized for many applications. The annual production of hydrous ferrous sulfate has been estimated to exceed 300 million tons in China [6]. Microemulsion method, Sol-Gel method, hydrothermal process, hydrolysis, flame pyrolysis and calcinations are employed popularly in the preparation of iron oxide powder from the hydrous ferrous sulfate [7–10]. Prim et al. have reported synthesis of hematite pigment from a steel industry waste with calcining at 1050 to 1200°C for 2 h [11]. Zheng Dianmo et al. [6] have reported preparation of nano ferric oxide from ferrous sulfate by liquid phase method. Majority of the reported methods demands an intermediate calcinations step at temperature above 400°C. Microwave heating finds wide application for drying of wide variety of material and for preparation of hematite. Dong Daihuan et al. [12] reported preparation of uniform β -FeO(OH) colloidal particles by hydrolysis of ferric salt using microwave heating, highlighting the increase in reaction rate and promotion of homogeneous nucleation. However, report related to calcination process of ferrous sulfate by microwave heating is limited.

It is well known that the size and shape of hematite powder has great impact on their application properties. The presence of surfactants and process temperature play an important role in the synthesis of hematite powders. High temperature increases the crystal growth rate as a result of agglomeration.

This paper aimed to prepare hematite using hydrous ferrous sulfate and investigate the effect of microwave heating on the structure and morphology of the product compared with the conventional method. The products

were obtained by decomposition reactions and the behavior of raw was informed by thermal analysis. Differences in the components, structures and particles of products were discussed based on the X-ray diffraction analysis, scan electron microscopy and particle analysis.

2 Experimental

2.1 Material

The hydrous ferrous sulfate used in the experiments was received from Panzhihua city, Sichuan province, China. It was the by-product in the process of production of titanium white powder. The chemical composition of hydrous ferrous sulfate is listed in Table 1. XRD was used to analyze the mineralogical content of the material (Fig. 1). The result indicated that rozenite and melanterite were the main crystalline compounds in the hydrous ferrous sulfate.

Constituent	Wt. %	Element	%
FeO	27.82	Fe	19.46
SO ₃	30.72	S	12.30
MgO	1.73	Mg	1.04
MnO	0.14	Mn	0.070
TiO ₂	0.18	Ti	0.108
Al ₂ O ₃	0.014	Al	0.0074
SiO ₂	≤0.005	Si	≤0.002
LOI (loss on ignition on 1000°C)	62.12	—	—

Table 1: Chemical composition of ferrous sulfate

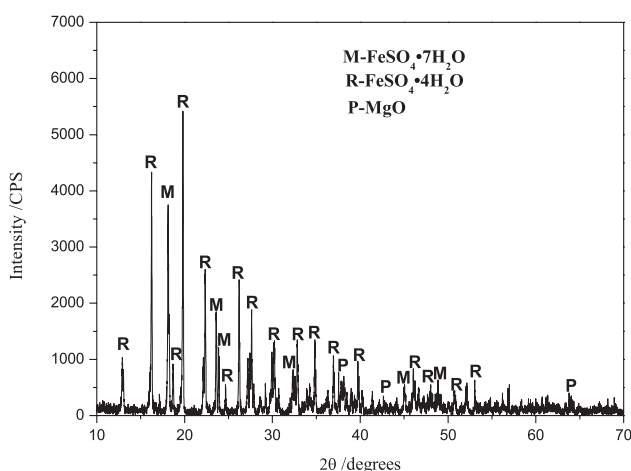


Fig. 1: The XRD profile of the raw material ferrous sulfate.

2.2 Characterization

The samples were characterized by Rigaku D/max-rc X-ray powder diffraction with Cu K α 1 ($\lambda = 1.54056 \text{ \AA}$, 40 kV, 200 mA, 10 deg/min).

Thermal behavior of the industrial ferrous sulfate was assessed by thermogravimetry and differentialthermogravimetry (TG and DTG) in presence of air. Thermal analysis measurements (TG-DTG) were carried out using thermal analyzer (NETZSCH STA 409, Germany), which include data acquisition and processing facility. The differential scanning calorimetry (DSC) measurement was carried out on analyzer (NETZSCH DSC 200, Germany). Thermal analysis experiments were conducted at a heating rate of 10°C/min, with a sample mass of 7.74 mg.

The morphology of Fe₂O₃ was characterized via scanning electron microscope (SEM) model (XL30, PHILIPS). The particles size, tested by laser particle size analyzer (RISE-2002, Jinan Runzhi, China), was analyzed to characterize the degree of agglomeration.

The total sulfur contents (TS) of samples was analyzed using iodine volume method according to Chinese standard GB/T14352.9-93.

2.3 Procedure and equipment

A microwave furnace (phoenix 905410, CEM, USA) and a conventional muffle furnace (KSY 15–16, Shanghai Y-Feng, China) were employed in the present work. Both the furnaces have advanced control system to maintain the desired calcination temperature and the heating rate. A sample mass of 40 g was utilized for each of the experimental runs. A heating rate of 20°C/min was adopted for both the modes of heating. All the experiments were conducted in presence of air with the furnace having good thermal insulation. The duration of each experiment after attaining the desired temperature was 25 min. The power to the furnace was terminated on completion of the experiment and the samples were allowed to cool down to the room temperature before being removed from the furnace.

3 Results and discussion

3.1 TG-DTG analysis

TG-DTG curves for non-isothermal decomposition in presence of air are presented in Fig. 2. The results indicate four

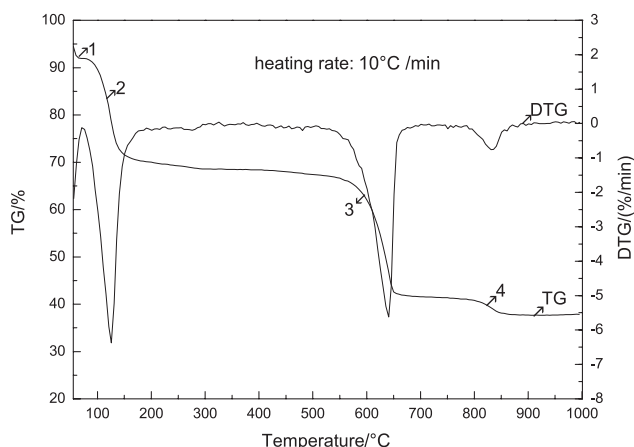


Fig. 2: TG/DTG curves of industrial ferrous sulfate in air.

weight loss steps (steps 1, 2, 3 and 4) in the TG curves, corresponding to the four peaks in DTG curves. The first and second steps are from 55 to 138°C, contributing to a weight loss of 30.37%, which is attributed to the dehydration of ferrous sulfate. The third step, which contributes to a weight loss of 25.85%, is owned to the oxidation and decomposition of ferrous sulfate, while the fourth step has a loss of 3.74%. A further increase in the TG temperature until 1000°C didn't show any significant weight changes, indicating the completion of decomposition and phase transition, which are in accordance with the literature reports [13]. Based on the weight loss pattern exhibited by the TG-DTG, the temperature for the thermal treatment was chosen in the present study.

3.2 DSC analysis

Fig. 3 illustrated the DSC curve of industrial ferrous sulfate in air at heating rate of 10°C/min. The DSC peaks were in well agreement with DTG peaks. According to the DSC curve the changes during the heating shows as in Table 2. The step 1 peak indicates an endothermic process that came down to melting and recrystallized. The step 2, step 3 and step 4 peaks indicates the exothermic process which was caused by the dehydration and decomposition.

3.3 Total sulfur analysis

Total sulfur contents of prepared products using conventional and microwave heating at different temperatures is shown in Table 3. The TS values decreased with the increase of the calcination temperature for both heating

DSC peak	Initial temperature/°C	Terminate temperature/°C	Peak temperature/°C
Step 1	50	105.4	75.7
Step 2	105.4	138.0	126.6
Step 3	606.5	649.1	640.0
Step 4	810.5	850.4	841.7

Table 2: Changes during heating according to the DSC analysis

Temperature/°C	TS/%	
	Convention	Microwave
650	18.46	18.23
750	7.71	2.44
850	4.90	0.12
950	3.86	–
1050	0.097	–

Table 3: Total sulfur of prepared sample

methods. By contrast, TS of 18.46% (convention) and 18.23% (microwave) at 650°C, as oppose to the initial TS of 12.30%, indicates the element of sulfur was still present in a large amount. The increase in the mass fraction of TS was attributed to a weight loss caused by removal of moisture. TS reduced significantly to 7.71% (convention) and 2.24% (microwave) at 750°C, due to the main decomposition step as evidenced in the TG-DTG curves. At 850°C only about 0.12% of sulfur remained with the sample using microwave heating, while 4.9% remained with the conventional heating, clearly indicating the effectiveness of the microwave heating process. The higher rate of decomposition of the ferrous sulfate could be attributed to the uniform and quick heating of the microwave heating process.

3.4 XRD analysis

Fig. 4a and 4b show the XRD patterns of samples prepared by conventional and microwave calcination at 650°C in presence of air, respectively. In both the modes of heating, the main phase is iron sulfate (JCPDS no. 42-0229). The peak positions of plane (012), (104), (110), (113), (024), (116), (214), and (300) for both samples matched consistently the stander data for hematite (JCPDS no. 33-0664), demonstrating the presence of α -Fe₂O₃. The chemical reaction for hematite synthesis illustrated as follow



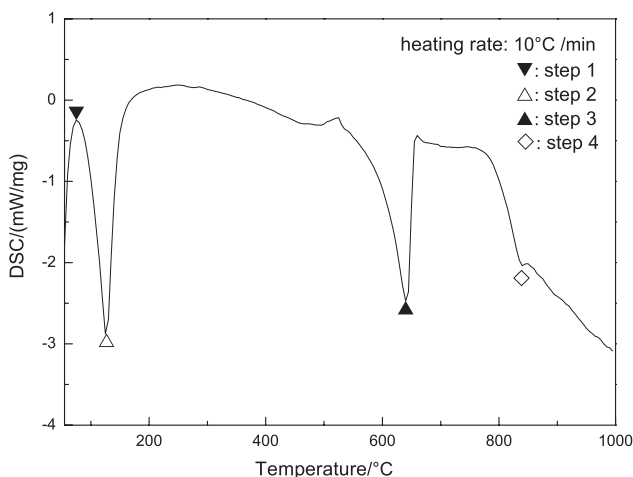


Fig. 3: DSC curve of industrial ferrous sulfate in air.

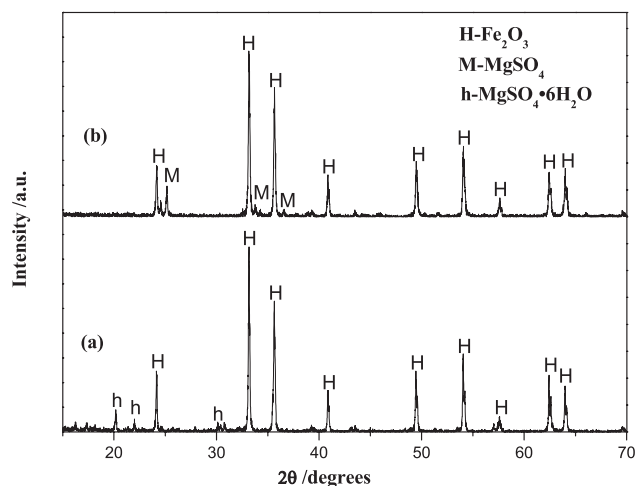


Fig. 5: XRD profiles of the products calcined at 750°C, (a) conventional calcinations and (b) microwave calcinations.

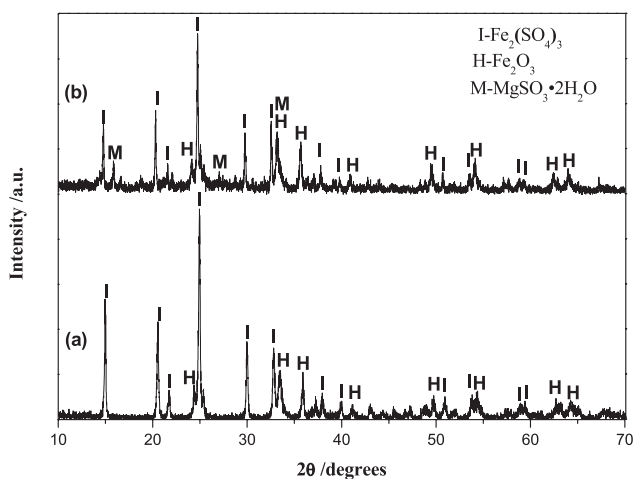
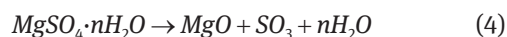


Fig. 4: XRD profiles of the products calcined at 650°C (a) conventional calcinations and (b) microwave calcinations.

This results indicate there is only a minor decomposition of $\text{Fe}_2(\text{SO}_4)_3$ at 650°C, which was consistent with the result reported in literature [14]. In this case, it is iron sulfate actually resulted the high TS values in samples (see in Table 2). While $\text{MgSO}_3 \cdot 2\text{H}_2\text{O}$ (JCPDS no. 11-0242) is only observed with microwave heating. The accidental observation of $\text{MgSO}_3 \cdot 2\text{H}_2\text{O}$ can be attributed to the transformation from the initial periclase and an interaction between the diverse impurities and the sulfur trioxide released through the decomposition.

The X-ray powder diffraction profiles of the products prepared at 750°C, respectively, using conventional and the microwave heating methods are shown in Fig. 5a and Fig. 5b. The main products in both heating modes were Fe_2O_3 (JCPDS no. 33-0664), which has a rhombohedrally centered hexagonal structure. However, the conventional

heating shows the presence of hematite along with a considerable amount of hexahydrate (JCPDS no. 24-0719), while the microwave heating only shows the presence of hematite and a minor quantity of magnesium sulfate (JCPDS no. 21-0546). The conventional heating shows large presence of hexahydrate, which clearly indicates the formation of hexahydrate prior to the formation of magnesium sulfate, as compared with microwave heating. The microwave heating indicates the completion of the decomposition process at 750°C evidenced from large presence of the hematite and absence of ferric sulfate, along with a minor presence of magnesium sulfate from the conversion of hexahydrate. The process of transformation of periclase during the calcinations can be explained as follow



The sulfur element of the magnesium sulfate came from the $\text{Fe}_2(\text{SO}_4)_3$ or from the sulfur dioxide atmosphere.

Fig. 6a and Fig. 6b displays the x-ray powder diffraction profiles of calcinations products at 850°C using conventional and microwave heating. The X-ray diffraction pattern of products satisfactorily matched with the standard values of hematite (JCPDS no. 33-0664), identifying clearly the primary crystals to be synthetic $\alpha\text{-Fe}_2\text{O}_3$ in Fig. 6a and Fig. 6b. Both of the diffraction peaks were sharp indicating the fine crystallization. As seen in Fig. 6a, several peaks occurred at 2θ values of 24.50°, 25.11°, 33.77° and 36.56°, corresponding to (021), (111), (022) and (130).

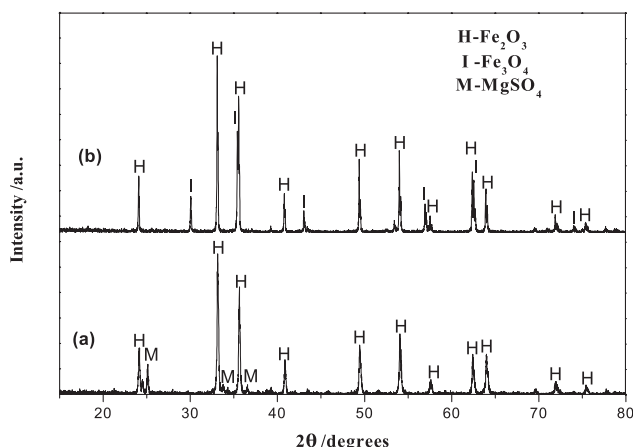


Fig. 6: XRD profiles of the products at 850°C, (a) conventional calcinations and (b) microwave calcinations.

These peaks matched well with the magnesium sulfate (JCPDS no. 21-0546). As seen in Fig. 6b, the diffraction peaks corresponding to plane of (220), (311), (400), (511) and (440) at 2θ values of 30.11° , 35.45° , 43.09° , 56.98° and 62.58° , matched the standard iron oxide (JCPDS no. 65-3107) perfectly, indicating the existence of a minor of iron oxide. The presence of magnesium sulfate in the conventional heating clearly indicates a conversion of hexahydrate (see in Fig. 5a) to magnesium sulfate. The absence of magnesium sulfate in the microwave heating indicates the completion of the decomposition, while the presence in the conventional heating could be attributed to the process in progress [15]. The higher amount of magnesium sulfate in the conventional heating can also be evidenced from the TS of 4.90% as compared to a 0.12% with microwave heating.

The microwave heating additionally shows the presence of iron oxide in Fig. 6b. The peaks was identified Fe_3O_4 instead of $\gamma\text{-Fe}_2\text{O}_3$, because of the absence of the characteristic reflection of plane (221) corresponding to $\gamma\text{-Fe}_2\text{O}_3$ [16, 17]. The formation of new crystal Fe_3O_4 could be attributed to conversion of primary hematite phase under reducing atmosphere and inadequate oxygen. The mixed presence of $\alpha\text{-Fe}_2\text{O}_3$ and Fe_3O_4 was also reported with the pH of solution in the range of 6–9 in literature [18]. Furthermore, the topotactic reaction has also been attributed to the transition of Fe_3O_4 , with both $\alpha\text{-Fe}_2\text{O}_3$ and Fe_3O_4 were still crystallite in rhombohedron [19].

3.5 Morphology and particle size of powder

Fig. 7a and Fig. 7b illustrates the morphology of the hematite powder obtained through the conventional and microwave heating, respectively. The hematite crystallite in Fig. 7a were irregular spherical particles with average diameter of 370 nm and were highly porous, possibly due to the uniform decomposition of $\text{Fe}_2(\text{SO}_4)_3$. Hematite with high porosity is also produced through the hydrolysis and calcinations in literature [20], attributed to the decomposition of FeCO_3 .

Fig. 7b revealed that the morphology of hematite prepared by microwave heating shown blocks of agglomerates which were irregular and non spherical in shape.

The average particle size distributions of hematite with conventional and microwave heating was presented in Fig. 8, with the average particle sizes being 1.3–2.1 μm (microwave) and about 17.58 μm (convention). Although there were agglomerates to some extent, the particles size

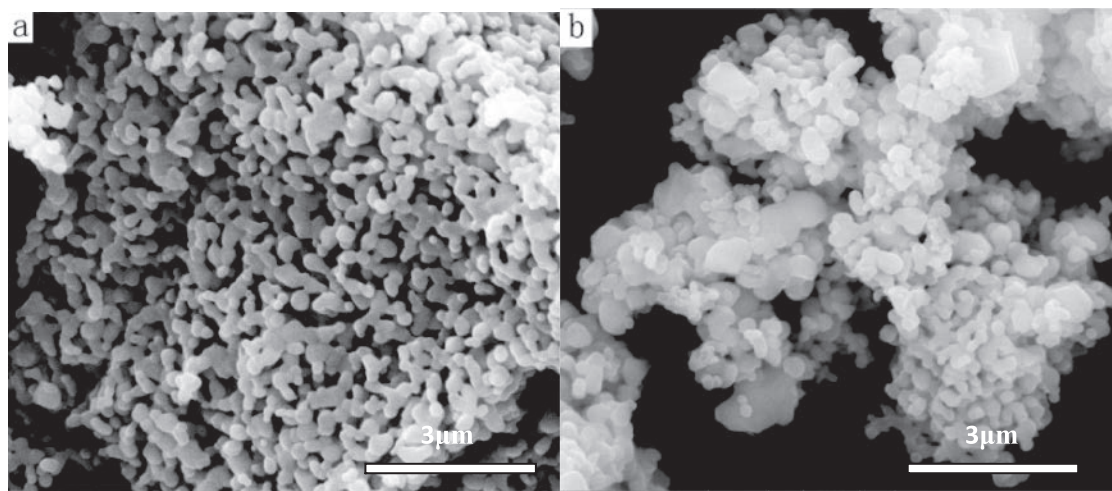


Fig. 7: SEM images of the hematite powder obtained at 850°C, (a) conventional method and (b) calcinations by microwave.

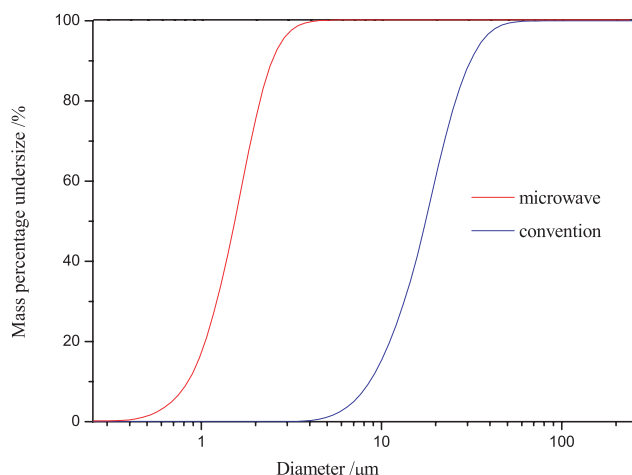


Fig. 8: Averaged size distributions of hematite calcined at 850°C.

of hematite by microwave heating was smaller than that of conventional heating. Formation of agglomerated hematite was also reported in literature [21], with average size of the spherical agglomerates being 0.15–0.2 μm or 1–5 μm at different pH values. The tendency to agglomerate to form crystalline particles of about 0.1 μm through direct precipitation was also reported by Dirk Walter [22].

4 Conclusion

Two heating methodologies were successfully developed to synthesize hematite powder using ferrous sulfate. This investigation aimed at identifying the difference of the quality of the product about major/minor phase and morphology. Increasing the reaction temperature, a minor of $\text{MgSO}_4 \cdot 6\text{H}_2\text{O}$ and MgSO_4 formed and then disappeared. By contrast, microwave played a strong effect in the decomposition of the ferric sulfate in terms of total sulfur content in the product decreased significantly. And the efficiency of decomposition was stronger with the microwave heating as all the sulfur compounds completely decomposed at 850°C. The micrometer scale particles about 1.3–2.1 μm have been prepared using microwave calcinations methods. Agglomeration seems to be inevitable with either microwave heating or conventional heating. This work highlighted the utilization of microwave heating for the preparation of hematite powder for potential applications in iron oxide and iron industry.

Acknowledgements: Financial supports from the National Natural Science Foundation of China (No.: 51090385).

Received: August 2, 2012. Accepted: October 29, 2012.

References

- [1] W.G. Yu, T.L. Zhang, J.G. Zhang, J.Y. Guo, R.F. Wu, *Prog. Chem.* 19 (2007), 885–890.
- [2] E.L. von Aderkas, M.M. Barsan, D.F.R. Gilson, I.S. Butler, *Spectrochim. Acta, part A*, 77 (2010), 954–959.
- [3] L.H. Huo, W. Li, L.H. Lu, H.N. Cui, S.Q. Xi, J. Wang, B. Zhao, Y.C. Shen, Z.H. Lu, *Chem. Mater.* 12 (2000), 790–794.
- [4] S. Wagloehner, D. Reichert, D.L. Sorzano, P. Balle, B. Geiger, S. Kureti, *J. Catal.* 260 (2008), 305–314.
- [5] L.S. Zhong, J.S. Hu, H.P. Liang, A.M. Cao, W.G. Song, L.J. Wan, *Adv. Mater.* 18 (2006), 2426–2431.
- [6] D.M. Zheng, F.I. Huang, X.R. Chen, J.H. Zheng, *Chem. Res. Appl.* 18 (2006), 840–843.
- [7] L.H. Han, H. Liu, W. Yu, *Powder Technol.* 207 (2011), 42–46.
- [8] P.P. Sarangi, B. Naik, N.N. Ghosh, *Powder Technol.* 192 (2009), 245–249.
- [9] Y.J. Zheng, Z.C. Liu, *Powder Technol.* 207 (2011), 335–342.
- [10] S. Grimm, T. Stelzner, J. Leuthäuser, S. Bartha, K. Heide, *Thermochim. Acta* 300 (1997), 141–148.
- [11] S.R. Prim, M.V. Folgueras, M.A. de Lima, D. Hotza, *J. Hazard. Mater.* 192 (2011), 1307–1313.
- [12] D.H. Dong, P.J. Hong, S.S. Dai, *Mater. Res. Bull.* 30 (1995), 537–541.
- [13] L. Machala, J. Tuček, R. Zbořil, *Chem. Mater.* 23 (2011), 3255–3272.
- [14] M.S.R. Swamy, T.P. Prasad, *Thermochim. Acta* 62 (1983), 229–236.
- [15] E. Alvarado, L.M. Torres-Martinez, A.F. Fuentes, P. Quirana, *Polyhedron* 19 (2000), 2345–2351.
- [16] S. Grimm, T. Stelzner, J. Leuthäuser, S. Barth, K. Heide, *Thermochim. Acta* 300 (1997), 141–148.
- [17] Y.B. Kholam, S.R. Dhage, H.S. Potdar, S.B. Deshpande, P.P. Bakare, S.D. Kulkarni, S.K. Date, *Mater. Lett.* 56 (2002), 571–577.
- [18] Y. Li, H. Liao, Y. Qian, *Mater. Res. Bull.* 33 (1998), 841–844.
- [19] B.W. Bailey, *Acta Cryst.* A33 (1977), 681–684.
- [20] S.Y. Lian, E. Wang, Z.H. Kang, Y.P. Bai, L. Gao, M. Jiang, C.W. Hu, L. Xu, *Solid State Commun.* 129 (2004), 485–490.
- [21] Y.B. Kholam, S.R. Dhage, H.S. Potdar, S.B. Deshpande, P.P. Bakare, S.D. Kulkarni, S.K. Date, *Mater. Lett.* 56 (2002), 571–577.
- [22] S.R. Dhage, Y.B. Kholam, H.S. Potdar, S.B. Deshpande, P.P. Bakare, S.R. Sainkar, S.K. Date, *Mater. Lett.* 57 (2002), 457–462.
- [23] D. Walter, *Thermochim. Acta* 445 (2006), 195–199.